HHS Public Access

Author manuscript

Knee Surg Sports Traumatol Arthrosc. Author manuscript; available in PMC 2020 July 12.

Published in final edited form as:

Knee Surg Sports Traumatol Arthrosc. 2020 July ; 28(7): 2124–2138. doi:10.1007/s00167-019-05685-y.

Anterior cruciate ligament grafts display differential maturation patterns on magnetic resonance imaging following reconstruction: a systematic review

Joseph A. Panos[1,2], **Kate E. Webster**[3], **Timothy E. Hewett**[2,4,5,6]

[1]Mayo Clinic Graduate School of Biomedical Sciences, Mayo Clinic, Rochester, MN, USA

[2]Department of Physiology and Biomedical Engineering, Mayo Clinic, 200 First St. SW, Rochester, MN 55902, USA

[3]School of Allied Health, La Trobe University, Melbourne, Australia

[4]Department of Orthopedic Surgery, Mayo Clinic, Rochester, MN, USA

[5]Mayo Clinic Biomechanics Laboratories and Sports Medicine Center, Mayo Clinic, Rochester, MN, USA

[6]Department of Physical Medicine and Rehabilitation, Mayo Clinic, Rochester, MN, USA

Abstract

Purpose—The appearance of anterior cruciate ligament (ACL) grafts on magnetic resonance imaging (MRI) is related to graft maturity and mechanical strength after ACL reconstruction (ACLR). Accordingly, the purpose of this review was to quantitatively analyze reports of serial MRI of the ACL graft during the first year following ACLR; the hypothesis tested was that normalized MRI signal intensity would differ significantly by ACL graft type, graft source, and postoperative time.

Methods—PubMed, Scopus, and CINAHL were searched for all studies published prior to June 2018 reporting MRI signal intensity of the ACL graft at multiple time points during the first postoperative year after ACLR. Signal intensity values at 6 and 12 months post-ACLR were normalized to initial measurements and analyzed using a least-squares regression model to study the independent variables of postoperative time, graft type, and graft source on the normalized MRI signal intensity.

Results—An effect of graft type ($P = 0.001$) with interactions of graft type * time ($P = 0.012$) and graft source * time ($P = 0.001$) were observed. Post hoc analyses revealed greater predicted

Timothy E. Hewett, Hewett.timothy@mayo.edu.

Author contributions TEH conceived the study, participated in the critical evaluation of the data and drafting of the manuscript. KEW participated in the critical evaluation of the data and drafting of the manuscript. JAP conducted the literature review, performed the critical evaluation of the data, and participated in the drafting and revision of the manuscript.

Conflict of Interest The authors declare that they have no conflict of interest.

Ethical approval Ethical approval was not required as this is a review of the literature not involving humans or animals.

Publisher's Note Springer Nature remains neutral with regard to jurisdictional claims in published maps and institutional affiliations.

normalized MRI signal intensity of patellar tendon autografts than both hamstring ($P = 0.008$) and hamstring with remnant preservation ($P = 0.001$) autografts at postoperative month 12.

Conclusion—MRI signal varies with graft type, graft source, and time after ACLR. Enhanced graft maturity during the first postoperative year was associated with hamstring autografts, with and without remnant preservation. Serial MRI imaging during the first postoperative year may be clinically useful to identify biologically or mechanically deficient ACL grafts at risk for failure.

Keywords

Anterior cruciate ligament; Magnetic resonance imaging; Signal–noise-quotient; Ligamentization

Introduction

The optimal graft source for anterior cruciate ligament (ACL) reconstruction (ACLR) remains controversial. Common tissues used for ACLR include semitendinosus and gracilis tendons, bone–patellar tendon–bone constructs, quadriceps tendon with or without patellar bone block, tibialis anterior, or tibialis posterior tendon grafts [19]. Furthermore, autogenous versus allogenic graft sources must be weighed in light of differences in cost [7], biological incorporation [22], and intra-articular functional adaptation [37].

After surgical reconstruction, ACL grafts undergo a sequential remodeling process termed ligamentization [5] which may be monitored by magnetic resonance imaging (MRI). The chronological postoperative changes to the graft begin with central hypocellularity without revascularization and normal cellularity and vascularity at the periphery [34]. A fibroblast and myofibroblast-driven proliferative phase subsequently occurs 6 weeks to 4 months after surgery [16, 34]. During this time, collagen orientation appears disorganized [1, 16, 34], reflecting a trough in mechanical strength. These extracellular matrix changes permit increased water molecule motion which corresponds to an increased signal on T2-weight MRI images [13]. Histologic maturation of the ACL graft follows, evidenced by collagen fibril alignment between 6 and 12 months [1, 36] with concurrent reports of hypo- [1] to hypervascularity [34, 36] for up to 3 years after surgery. The architectural changes to the ACL graft during this period promote T2 signal decay and low signal intensity on T2-weighted MRI images [11]. A fourth, quiescent phase has been reported at 3 years postoperatively, with cellularity and vascularity similar to the native ACL [34]. Thus, the ACL graft exhibits dynamic histological changes that produce measurable differences in MRI signals [9, 41].

Because the histological changes occurring during graft ligamentization may be evaluated by MRI, serial MRI in the postoperative period may offer non-invasive methods to monitor graft maturation in the clinical setting. Additionally, this knowledge of graft maturation patterns may inform pre-operative clinical decisions about graft type and source for ACLR. Previous investigations have described observational sequential MRI imaging in the postoperative period [18, 21, 32, 38], and a limited subset of reports directly compared imaging results by graft type [17, 24–26, 30] or graft source [12, 33]. Accordingly, the purpose of this study was to conduct a systematic review of MRI studies imaging the maturation of different types of ACL grafts from various sources during the first

postoperative year. The hypothesis tested was that there would be a significant effect of time, graft type, and graft source on normalized MRI signal intensity of the ACL graft.

Materials and methods

Search strategy

Electronic searches of PubMed, Scopus, and CINAHL databases were performed for all articles published prior to June 2018. A manual search of the reference lists was performed on studies identified for final inclusion in the systematic review. Publication lists derived from search criteria were stored in EndNote bibliographic software. The search strategy, inclusion and exclusion criteria are described in Table 1; the results of the literature search are depicted in Fig. 1. The tertiary review of studies for final inclusion was conducted and agreed upon by all authors.

Data extraction and synthesis

The primary outcome of interest was the MRI signal intensity of the ACL graft as a function of time after ACLR. Data were further analyzed by graft type: (1) bone–patellar tendon–bone graft (BPTB); (2) hamstring graft (HS); (3) hamstring graft with minimal debridement/remnant preservation surgical technique (HS-RP); (4) tibialis anterior graft (TA); and (5) quadriceps bone graft (QUAD) and by graft source: (1) autologous; and (2) allogenic.

Data analysis

In humans, the remodeling phase of the ACL graft has been reported to begin at 3 [34], 5 [1], 6 [16], or 12 [36] months after ACLR. To capture the full spectrum of graft remodeling, MRI signal intensity data were recorded at three time points for each study: the earliest reported time period closest to 3 months, at 6 months, and at 12 months. The normalized MRI signal intensity was calculated as the quotient of the MRI signal intensity of the 6 or 12 month time point divided by the MRI signal intensity at the initial time point. A ratio greater than 1 reflects an increase in the normalized MRI signal intensity away from graft maturity; a ratio less than 1 reflects a decrease in the normalized MRI signal intensity towards graft maturity.

Development of an MRI signal intensity prediction model

Statistical analyses were performed in JMP 13 (SAS Institute). For each data point, normalized MRI signal intensity values, graft type, graft source, time point, and the corresponding number of imaged patients were recorded. A weighted least-squares regression model using independent variables of graft type, graft source, and time point was constructed to generate predicted normalized MRI signal intensity values at 6 and 12 months. The number of patients imaged at each data point was used as a weight in the model. Analysis of variance (ANOVA) testing was performed on the predicted normalized MRI signal intensity values at 6 and 12 months. Post hoc 2 sample Student's t tests were performed on predicted normalized MRI signal intensities between graft types and graft sources; 1 sample Student's t tests were performed on predicted normalized MRI signal intensities for each graft source between graft types at each time point to assess the change from the normalized ratio of 1. $P < 0.05$ was established for statistical significance.

Effect size meta–analysis

To compare the trends in predicted normalized MRI signal intensity, mean effect sizes and 95% confidence intervals (CI) for the difference from baseline for the 6 and 12 month time period and the difference between the 12 and 6 month normalized MRI signal intensity data were calculated for BPTB, HS, and HS-RP autografts. The effect size for each study was calculated using an effect size meta-analysis with random effects model using Stats Direct Software (Version 2.8, Altrincham, U.K.). Where no measures of variability were reported, the mean standard deviation from other trials that reported this statistic was imputed. This imputation was performed only for the Gohil et al. study.

Quality assessment

Methodologic quality of the studies included in the quantitative analysis was assessed using a 27 item checklist for methodological and reporting quality of both randomized and non-randomized studies of healthcare interventions [14].

Results

Data pooling

A total of 412 subjects at initial time points, 397 at 6 months, and 388 at 12 months were pooled for the quantitative analysis. MRI scans of 590 HS autografts (initial: $N = 197$; 6 month: $N = 196$; 12 month: $N = 197$), 60 HS allografts (initial: $N = 20$; 6 month: $N = 20$; 12 month: $N = 20$), 112 for HS-RP autografts (initial: $N = 41$; 6 month: $N = 37$; 12 month: $N = 34$), 236 BPTB autografts (initial: $N = 77$; 6 month: $N = 77$; 12 month: $N = 82$), 72 BPTB allografts (initial: $N = 24$; 6 month: $N = 24$; 12 month: $N = 24$), 76 QUAD autografts (initial: $N = 36$; 6 month: $N = 26$; 12 month: $N = 14$), and 51 TA allografts (initial: $N = 17$; 6 month: $N = 17$; 12 month: $N = 17$) were included in the analysis. A summary of the twelve pooled studies included in the quantitative analysis, with MRI acquisition sequences and image analysis methods, is provided in Table 2.

Six studies reported a signal-to-noise quotient (SNQ) calculated at a discrete point at the intra-articular portion of the ACL graft [12, 17, 24, 30, 33, 38], one study reported the SNQ as an average of the proximal, middle, and distal intra-articular portions of the ACL graft [26], one study reported the SNQ as the average of a region of interest that encompassed the entire intra-articular portion of the ACL graft [18], and four studies reported the raw signal intensity of the mid-substance or intra-articular portion of the ACL graft [20, 21, 25, 32]. The initial time point for 12 of the 16 experimental groups included in the quantitative analysis corresponded to 3 months. For two studies, which corresponded to four experimental groups and 94 subjects, the MRI signal data were normalized to 2 [17] and 4 [33] month time points, which were the earliest reported time period closest to 3 months.

Regression modeling

The model equation and fit for predicted normalized MRI signal intensity are given in Fig. 2. The predicted normalized MRI signal intensity at 6 months was 1.05 ± 0.11, 1.08 ± 0.08, 0.48 ± 0.18, and 0.86 ± 0.21 for BPTB, HS, HS-RP, and QUAD autografts, respectively ($P = 0.013$). Post hoc t test revealed significantly decreased predicted normalized MRI signal

intensity for HS-RP compared to BPTB ($P = 0.013$) and HS ($P = 0.005$) autografts; no differences were observed between BPTB and HS autografts (n.s.). The predicted normalized MRI signal intensity at 12 months was 1.20 ± 0.12, 0.81 ± 0.08, 0.40 ± 0.18, and 0.94 ± 0.27 for BPTB, HS, HS-RP, and QUAD autografts, respectively ($P = 0.004$). Post hoc *t* tests revealed significantly increased predicted normalized MRI signal intensity for BPTB grafts compared to HS ($P = 0.008$) and HS-RP ($P = 0.001$). At postoperative month 12, the predicted normalized MRI signal intensity of HS grafts was significantly less than the initial value ($P = 0.021$). The predicted normalized MRI signal intensity of the HS-RP graft was significantly less than the initial value at 6 ($P = 0.008$) and 12 ($P = 0.003$) months. Between 6 and 12 months, predicted normalized MRI signal intensity of HS grafts decreased ($P = 0.018$); no changes between 6 and 12 months were observed for BPTB (n.s.), QUAD (n.s.), or HS-RP (n.s.) autografts (Fig. 3).

The predicted normalized MRI signal intensity at 6 months was 1.05 ± 0.11, 1.08 ± 0.08, and 2.08 ± 0.25 for BPTB, HS, and TA allografts, respectively ($P < 0.001$). Post hoc *t* tests revealed significantly increased predicted normalized MRI signal intensity for TA compared to BPTB ($P = 0.001$) and HS ($P < 0.001$) allografts; no differences were observed between BPTB and HS allografts (n.s.). At postoperative month 12, predicted normalized MRI signal intensity was 1.82 ± 0.17, 1.43 ± 0.17, and 1.28 ± 0.25 for BPTB, HS, and TA allografts, respectively (n.s.). Between 6 and 12 months, predicted normalized MRI signal intensity of BPTB increased ($P < 0.001$), TA decreased ($P = 0.017$), and HS did not significantly change ($P = 0.072$) (Fig. 4).

Effect size

The mean effect size for the difference in normalized MRI signal intensity between 6 months and baseline was 0.0004 (CI − 0.711–0.711; n.s.), − 1.295 (CI − 2.079–0.511; $P = 0.001$), and 0.108 (CI − 0.453–0.669; n.s.) for HS autografts, HS-RP autografts, and BPTB autografts, respectively (Fig. 5a–c). The mean effect size for the difference between 12 months and baseline was − 0.525 (CI − 1.356–0.306; n.s.), −1.285 (CI − 2.216–0.355; $P = 0.007$), and 0.743 (CI − 0.584–2.069; n.s.) for HS autografts, HS-RP autografts, and BPTB autografts, respectively (Fig. 5d–f). The mean effect size for the difference between 12 and 6 months in HS autografts, HS-RP autografts, and BPTB autografts was − 0.562 (CI − 0.825–0.301; $P < 0.001$), − 0.070 (CI − 0.537–0.397; n.s.), and 0.572 (CI − 0.275–1.420; n.s.) (Fig. 5g–i).

Quality

Quality assessment scores ranged from 12 to 23 (of a possible 28). While the vast majority of studies were adequate in their reporting measures, only two [12, 26] of the twelve studies included power analyses, illustrating the uncertainty in defining statistically and, more importantly, clinically significant effects in postoperative imaging measures (Table 2).

Discussion

This study demonstrates that the postoperative MRI appearance of the ACL changes with time after reconstructive surgery and differs by ACL graft type and graft source. The effect

of individual and interactional variables graft type, graft source, and time after reconstruction on the normalized MRI signal was determined by the development and utilization of a least-squares regression model. Between postoperative months 6 and 12, the predicted normalized MRI signal intensity for HS autografts significantly decreased, while BPTB allograft signal significantly increased. By 12 months, BPTB autograft predicted normalized MRI signal intensity was significantly greater than HS and HS-RP autograft values. Predicted normalized MRI signal intensity for HS and HS-RP autografts were significantly less than initial values by 12 months.

Graft type

Histologic irregularities in collagen orientation, which may influence MRI signal, persist at 12 months after ACLR in HS and BPTB grafts [23]. The distribution of collagen fibril size in HS grafts is unimodal at 1 year postoperatively, which is distinct from both the native ACL and BPTB grafts [42, 43]. Neovascularization occurs at 3 weeks in autogenous BPTB grafts [35] with focal areas of acellularity at 8 weeks, and degeneration at 6–10 months, resolving at 1–3 years postoperatively [34]. The current MRI imaging results and well characterized histological changes to HS grafts support relatively static remodeling during the first postoperative year. Conversely, the increased MRI signal of BPTB grafts at 1 year observed in this study, in addition to histologic reports of BPTB grafts, could represent a remodeling state of the graft due to dynamic cellular, vascular, and tissue changes.

HS-RP autografts were associated with decreased normalized MRI signal at 6 and 12 months. Preservation of the ACL remnant has been hypothesized to promote revascularization of the ACL graft and accelerated progression through ligamentization [3, 6, 39]; however, to the authors' knowledge, no human studies have correlated MRI findings with graft histology. While the inclusion of multiple studies in this review may allow for greater power to observe a difference in HS-RP grafts, it is possible that the 3 month time point to which MRI signal data were normalized represents an early, revascularized stage for HS-RP grafts after which time the graft matures and remodels to establish a low signal intensity structure with high mechanical strength. Thus, the lower predicted normalized MRI signal intensities observed in HS-RP grafts may represent maturation from the initial 3 month time point, possibly due to the contribution of the ACL remnant.

Graft source

Previous studies using MRI to measure graft maturity report differences between allografts and autografts [28]. Contrast-enhanced MRI revealed elevated MRI signal between 4 and 6 months for autografts and persistently elevated signal from 4 to 24 months in allografts [33]; these MRI imaging differences suggest delayed re-establishment of vascularity in allografts compared to autografts, which may impede ligamentization. These findings are corroborated histologically in post-mortem ACL allograft retrieval studies that demonstrate areas of acellularity 2 years postoperatively [31]. Thus, allogeneic grafts may undergo incomplete or delayed revascularization that hinders cellular repopulation and tissue re-organization, manifested as an increased MRI signal intensity, as reported in this study. Conversely, an autologous graft source may promote accelerated graft maturity, possibly through earlier and complete revascularization, and allow for sequential progression and completion of

ligamentization. Due to known differences in vascularization, cellular repopulation, MRI signal intensity, and clinical rates of failure between allografts and autografts, future studies should examine the possible mechanisms, immunological or otherwise, which cause these findings.

Effect sizes and model comparisons

The trends predicted by the least-squares regression model were generally mirrored in the calculation of effect sizes from sample data. The model was able to replicate accurately the majority of trends for normalized MRI graft signal intensity for HS, BPTB, and HS-RP autografts. In one instance, the effect size for HS autografts did not differ significantly from the initial measurement at 12 months (Fig. 5e), but the predicted normalized MRI signal intensity for HS autografts was significantly lower than initial values at 12 months (Fig. 3). The observed difference could be due to the standard deviation of initial normalized MRI signal intensity values, accounted for the effect size calculation.

This study had multiple limitations. First, graft SNQ is influenced by anatomic factors, knee position within the MRI machine [15, 27], surgical technique [4], and graft bending angle [2, 20, 40]. These differences could confound MRI signal intensity measurements, limiting MRI as a quantitative method to measure graft maturation. Second, the heterogeneity of methods in measuring signal intensities prevented the direct comparison between studies, graft types, and graft sources; however, normalization of reported signal intensity values for each study allowed for the comparison of general trends in graft appearance on MRI during the first postoperative year. Finally, the signal intensity of MRI is influenced by multiple technical factors, which include sequence and scanner characteristics, reconstruction algorithms, and grey scale displays [10]. This limitation is mitigated by the use of a uniform imaging protocol, pulse sequence, and static magnetic field for each of the studies included in this review.

The clinical utility of graft maturation assessment via MRI is becoming increasingly recognized. Measurement of the MRI signal of the ACL graft in the sixth month after surgery predicts patient-reported outcomes of knee function at both 6 and 12 months postoperatively [29]. At longer follow-up periods of 3 and 5 years, MRI measurements of graft volume and signal intensity predict 1-legged hop test performance and patient-reported measures of knee function and symptomatology [8]. The results of this study support previous reports that the MRI signal intensity of the ACL graft varies as a function of time, and further suggest significant differences by graft type and graft source. Future work to associate graft-specific differences in MRI signal intensity with appropriate clinical correlates could inform preoperative clinical decision making regarding graft selection, progression through rehabilitation protocols, as well as the decision to return to preoperative levels of activity.

Conclusion

Serial MRI of the ACL graft during the first year after ACLR demonstrates that graft type, graft source, and time after implantation affect the normalized MRI signal intensity of ACL transplants. Hamstring autograft source, with and without remnant preservation, was

associated with significantly decreased predicted normalized MRI signal intensity at postoperative month 12, below BPTB and initial values. The observed trends for the predicted normalized MRI signal intensity of HS and BPTB grafts correlate with histological reports in the literature. Thus, MRI imaging may be a useful clinical measure to monitor graft-specific remodeling after ACLR and better knowledge of graft-specific maturation patterns may inform preoperative decisions regarding graft source and selection.

Funding

Funding was provided by National Institute of Arthritis and Musculoskeletal and Skin Diseases (Grant Nos. R01AR55563, R01AR056259 and T32AR56950).

Abbreviations

ACL	Anterior cruciate ligament
ACLR	Anterior cruciate ligament reconstruction
MRI	Magnetic resonance imaging
BPTB	Bone–patellar tendon–bone graft
HS	Hamstring graft
HS-RP	Hamstring graft with minimal debridement/remnant preservation surgical technique
TA	Tibialis anterior graft
QUAD	Quadriceps bone graft
ANOVA	Analysis of variance
CI	Confidence interval
SNQ	Signal-to-noise quotient

References

1. Abe S, Kurosaka M, Iguchi T, Yoshiya S, Hirohata K (1993) Light and electron microscopic study of remodeling and maturation process in autogenous graft for anterior cruciate ligament reconstruction. Arthroscopy 9:394–405 [PubMed: 8216570]
2. Ahn JH, Jeong HJ, Lee YS, Park JH, Lee JH, Ko TS (2016) Graft bending angle is correlated with femoral intraosseous graft signal intensity in anterior cruciate ligament reconstruction using the outside-in technique. Knee 23:666–673 [PubMed: 26968485]
3. Ahn JH, Lee SH, Choi SH, Lim TK (2010) Magnetic resonance imaging evaluation of anterior cruciate ligament reconstruction using quadrupled hamstring tendon autografts: comparison of remnant bundle preservation and standard technique. Am J Sports Med 38:1768–1777 [PubMed: 20805412]
4. Ahn JH, Lee YS, Jeong HJ, Park JH, Cho Y, Kim KJ et al. (2017) Comparison of transtibial and retrograde outside-in techniques of anterior cruciate ligament reconstruction in terms of graft nature and clinical outcomes: a case control study using 3T MRI. Arch Orthop Trauma Surg 137:357–365 [PubMed: 28132087]

5. Amiel D, Kleiner JB, Roux RD, Harwood FL, Akeson WH (1986) The phenomenon of "ligamentization": anterior cruciate ligament reconstruction with autogenous patellar tendon. J Orthop Res 4:162–172 [PubMed: 3712125]
6. Arnoczky SP, Tarvin GB, Marshall JL (1982) Anterior cruciate ligament replacement using patellar tendon. An evaluation of graft revascularization in the dog. J Bone Jt Surg Am 64:217–224
7. Barrera Oro F, Sikka RS, Wolters B, Graver R, Boyd JL, Nelson B et al. (2011) Autograft versus allograft: an economic cost comparison of anterior cruciate ligament reconstruction. Arthroscopy 27:1219–1225 [PubMed: 21820267]
8. Biercevicz AM, Akelman MR, Fadale PD, Hulstyn MJ, Shalvoy RM, Badger GJ et al. (2015) MRI volume and signal intensity of ACL graft predict clinical, functional, and patient-oriented outcome measures after ACL reconstruction. Am J Sports Med 43:693–699 [PubMed: 25540298]
9. Biercevicz AM, Miranda DL, Machan JT, Murray MM, Fleming BC (2013) In Situ, noninvasive, T2*-weighted MRI-derived parameters predict ex vivo structural properties of an anterior cruciate ligament reconstruction or bioenhanced primary repair in a porcine model. Am J Sports Med 41:560–566 [PubMed: 23348076]
10. Bloem JL, Reijnierse M, Huizinga TWJ, van der Helm-van Mil AHM (2018) MR signal intensity: staying on the bright side in MR image interpretation. RMD Open 4:e000728 [PubMed: 29955387]
11. Blumenkrantz G, Majumdar S (2007) Quantitative magnetic resonance imaging of articular cartilage in osteoarthritis. Eur Cell Mater 13:76–86 [PubMed: 17506024]
12. Chen L, Wu Y, Lin G, Wei P, Ye Z, Wang Y et al. (2018) Graft bending angle affects allograft tendon maturity early after anterior cruciate ligament reconstruction. Knee Surg Sports Traumatol Arthrosc. 10.1007/s00167-018-4910-x
13. Choi JA, Gold GE (2011) MR imaging of articular cartilage physiology. Magn Reson Imaging Clin N Am 19:249–282 [PubMed: 21665090]
14. Downs SH, Black N (1998) The feasibility of creating a checklist for the assessment of the methodological quality both of randomised and non-randomised studies of health care interventions. J Epidemiol Community Health 52:377–384 [PubMed: 9764259]
15. Echigo J, Yoshioka H, Takahashi H, Niitsu M, Fukubayashi T, Itai Y (1999) Signal intensity changes in anterior cruciate ligament autografts: relation to magnetic field orientation. Acad Radiol 6:206–210 [PubMed: 10894077]
16. Falconiero RP, DiStefano VJ, Cook TM (1998) Revascularization and ligamentization of autogenous anterior cruciate ligament grafts in humans. Arthroscopy 14:197–205 [PubMed: 9531133]
17. Gohil S, Annear PO, Breidahl W (2007) Anterior cruciate ligament reconstruction using autologous double hamstrings: a comparison of standard versus minimal debridement techniques using MRI to assess revascularisation. A randomised prospective study with a one-year follow-up. J Bone Jt Surg Br 89:1165–1171
18. Hakozaki A, Niki Y, Enomoto H, Toyama Y, Suda Y (2015) Clinical significance of T2*-weighted gradient-echo MRI to monitor graft maturation over one year after anatomic double-bundle anterior cruciate ligament reconstruction: a comparative study with proton density-weighted MRI. Knee 22:4–10 [PubMed: 25482345]
19. Houck DA, Kraeutler MJ, Vidal AF, McCarty EC, Bravman JT, Wolcott ML et al. (2018) Variance in anterior cruciate ligament reconstruction graft selection based on patient demographics and location within the multicenter orthopaedic outcomes network cohort. J Knee Surg 31:472–478 [PubMed: 28701007]
20. Howell SM, Berns GS, Farley TE (1991) Unimpinged and impinged anterior cruciate ligament grafts: MR signal intensity measurements. Radiology 179:639–643 [PubMed: 2027966]
21. Hsu CJ, Hsu HC, Jim YF (2003) A radiological study after anterior cruciate ligament reconstruction. J Chin Med Assoc 66:160–165 [PubMed: 12779036]
22. Jackson DW, Grood ES, Goldstein JD, Rosen MA, Kurzweil PR, Cummings JF et al. (1993) A comparison of patellar tendon autograft and allograft used for anterior cruciate ligament reconstruction in the goat model. Am J Sports Med 21:176–185 [PubMed: 8465909]

23. Janssen RP, van der Wijk J, Fiedler A, Schmidt T, Sala HA, Scheffler SU (2011) Remodelling of human hamstring autografts after anterior cruciate ligament reconstruction. Knee Surg Sports Traumatol Arthrosc 19:1299–1306 [PubMed: 21293848]
24. Lee BI, Kim BM, Kho DH, Kwon SW, Kim HJ, Hwang HR (2016) Does the tibial remnant of the anterior cruciate ligament promote ligamentization? Knee 23:1133–1142 [PubMed: 27806877]
25. Lee S, Seong SC, Jo CH, Han HS, An JH, Lee MC (2007) Anterior cruciate ligament reconstruction with use of autologous quadriceps tendon graft. J Bone Jt Surg Am 89(Suppl 3):116–126
26. Li H, Chen J, Li H, Wu Z, Chen S (2017) MRI-based ACL graft maturity does not predict clinical and functional outcomes during the first year after ACL reconstruction. Knee Surg Sports Traumatol Arthrosc 25:3171–3178 [PubMed: 27485123]
27. Li H, Chen S, Tao H, Li H, Chen S (2014) Correlation analysis of potential factors influencing graft maturity after anterior cruciate ligament reconstruction. Orthop J Sports Med 2:2325967114553552 [PubMed: 26535275]
28. Li H, Tao H, Cho S, Chen S, Yao Z, Chen S (2012) Difference in graft maturity of the reconstructed anterior cruciate ligament 2 years postoperatively: a comparison between autografts and allografts in young men using clinical and 3.0-T magnetic resonance imaging evaluation. Am J Sports Med 40:1519–1526 [PubMed: 22495290]
29. Li Q, Zhang Y, Zhan L, Han Q, Wu M, Zhang N (2019) Correlation analysis of magnetic resonance imaging-based graft maturity and outcomes after anterior cruciate ligament reconstruction using international knee documentation committee score. Am J Phys Med Rehabil 98:387–391 [PubMed: 30702461]
30. Liu S, Li H, Tao H, Sun Y, Chen S, Chen J (2018) A randomized clinical trial to evaluate attached hamstring anterior cruciate ligament graft maturity with magnetic resonance imaging. Am J Sports Med 46:1143–1149 [PubMed: 29443537]
31. Malinin TI, Levitt RL, Bashore C, Temple HT, Mnaymneh W (2002) A study of retrieved allografts used to replace anterior cruciate ligaments. Arthroscopy 18:163–170 [PubMed: 11830810]
32. Min BH, Chung WY, Cho JH (2001) Magnetic resonance imaging of reconstructed anterior cruciate ligament. Clin Orthop Relat Res 393:237–243
33. Muramatsu K, Hachiya Y, Izawa H (2008) Serial evaluation of human anterior cruciate ligament grafts by contrast-enhanced magnetic resonance imaging: comparison of allografts and autografts. Arthroscopy 24:1038–1044 [PubMed: 18760212]
34. Rougraff B, Shelbourne KD, Gerth PK, Warner J (1993) Arthroscopic and histologic analysis of human patellar tendon autografts used for anterior cruciate ligament reconstruction. Am J Sports Med 21:277–284 [PubMed: 8465925]
35. Rougraff BT, Shelbourne KD (1999) Early histologic appearance of human patellar tendon autografts used for anterior cruciate ligament reconstruction. Knee Surg Sports Traumatol Arthrosc 7:9–14 [PubMed: 10024956]
36. Sanchez M, Anitua E, Azofra J, Prado R, Muruzabal F, Andia I (2010) Ligamentization of tendon grafts treated with an endogenous preparation rich in growth factors: gross morphology and histology. Arthroscopy 26:470–480 [PubMed: 20362825]
37. Scheffler SU, Schmidt T, Gangey I, Dustmann M, Unterhauser F, Weiler A (2008) Fresh-frozen free-tendon allografts versus autografts in anterior cruciate ligament reconstruction: delayed remodeling and inferior mechanical function during long-term healing in sheep. Arthroscopy 24:448–458 [PubMed: 18375278]
38. Stöckle U, Hoffmann R, Schwedke J, Lubrich J, Vogl T, Südkamp NP et al. (1998) Anterior cruciate ligament reconstruction: the diagnostic value of MRI. Int Orthop 22:288–292 [PubMed: 9914930]
39. Takahashi T, Kimura M, Hagiwara K, Ohsawa T, Takeshita K (2018) The effect of remnant tissue preservation in anatomic double-bundle ACL reconstruction on knee stability and graft maturation. J Knee Surg. 10.1055/s-0038-1660513

40. Tashiro Y, Gale T, Sundaram V, Nagai K, Irrgang JJ, Anderst W et al. (2017) The graft bending angle can affect early graft healing after anterior cruciate ligament reconstruction. in vivo analysis with 2 years' follow-up. Am J Sports Med 45:1829–1836 [PubMed: 28402758]

41. Weiler A, Peters G, Maurer J, Unterhauser FN, Sudkamp NP (2001) Biomechanical properties and vascularity of an anterior cruciate ligament graft can be predicted by contrast-enhanced magnetic resonance imaging. A two-year study in sheep. Am J Sports Med 29:751–761 [PubMed: 11734489]

42. Zaffagnini S, De Pasquale V, Marchesini Reggiani L, Russo A, Agati P, Bacchelli B et al. (2010) Electron microscopy of the remodelling process in hamstring tendon used as ACL graft. Knee Surg Sports Traumatol Arthrosc 18:1052–1058 [PubMed: 19787336]

43. Zaffagnini S, De Pasquale V, Marchesini Reggiani L, Russo A, Agati P, Bacchelli B et al. (2007) Neoligamentization process of BTPB used for ACL graft: histological evaluation from 6 months to 10 years. Knee 14:87–93 [PubMed: 17188877]

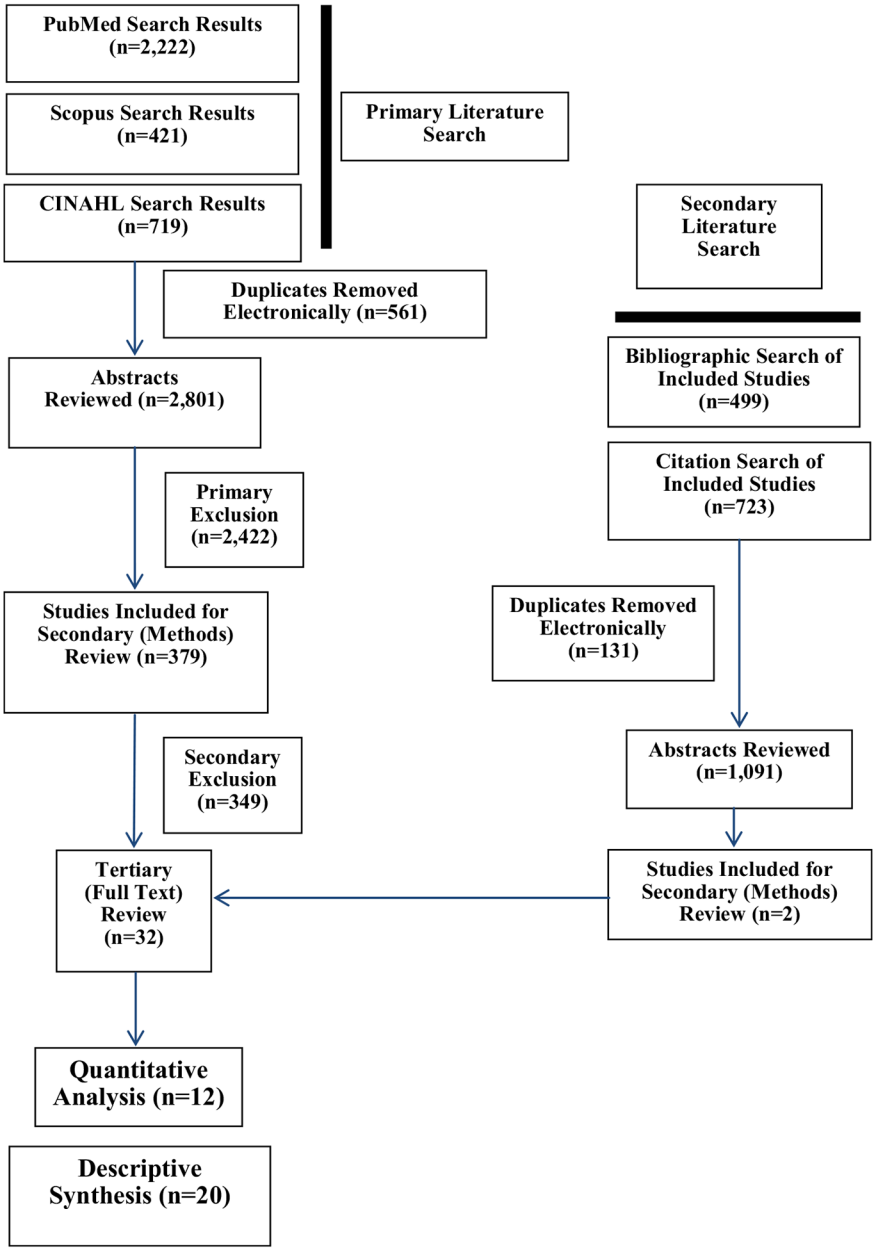

Fig. 1.

Literature search results. The most common reason for final exclusion from the quantitative analysis during tertiary review was the lack of serial imaging studies during the first postoperative year (descriptive synthesis; $N = 20$). Accordingly, all studies included in the quantitative analysis ($N = 12$) reported imaging studies at multiple time points during the first postoperative year

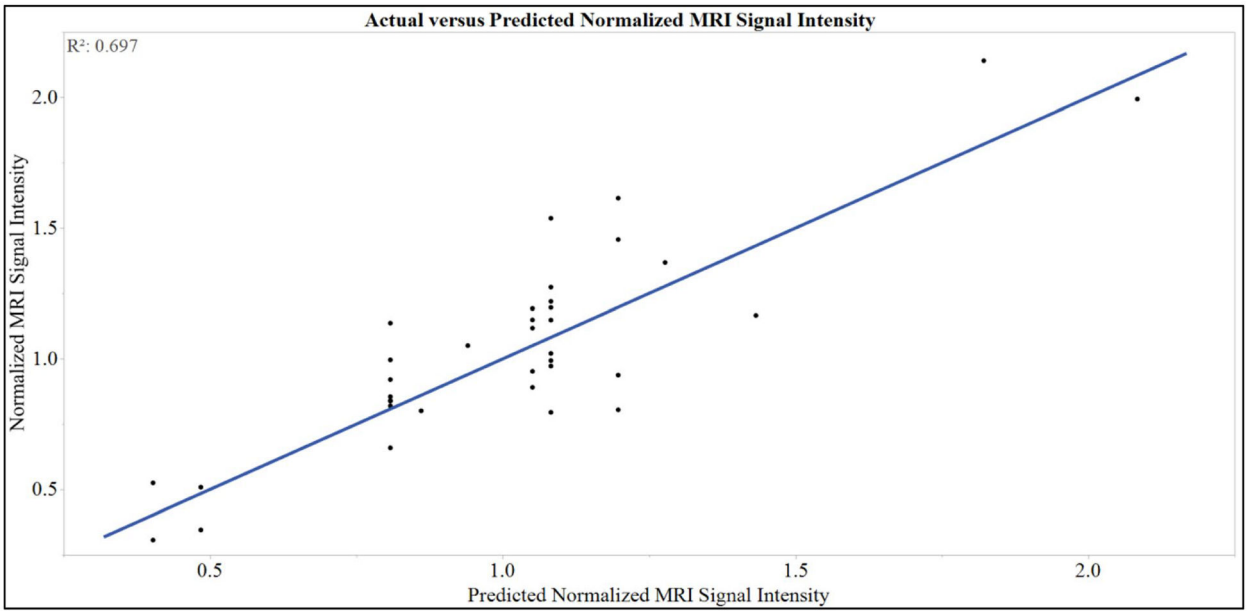

Predicted Normalized MRI Signal Intensity

$$= 1.112 + \begin{bmatrix} \text{BPTB} & -0.062 \\ \text{HS} & -0.030 \\ \text{HS} - \text{RP} & -0.628 \\ \text{QUAD} & -0.252 \\ \text{TA} & 0.972 \end{bmatrix} + \begin{bmatrix} \text{BPTB} \overset{\text{Match}}{\Longrightarrow} \begin{bmatrix} 6\text{ mo.} = 0 \\ 12\text{ mo.} = 0.459 \end{bmatrix} \\ \text{HS} \overset{\text{Match}}{\Longrightarrow} \begin{bmatrix} 6\text{ mo.} = 0 \\ 12\text{ mo.} = 0.038 \end{bmatrix} \\ \text{HS} - \text{RP} \overset{\text{Match}}{\Longrightarrow} \begin{bmatrix} 6\text{ mo.} = 0 \\ 12\text{ mo.} = 0.231 \end{bmatrix} \\ \text{QUAD} \overset{\text{Match}}{\Longrightarrow} \begin{bmatrix} 6\text{ mo.} = 0 \\ 12\text{ mo.} = 0.392 \end{bmatrix} \\ \text{TA} \overset{\text{Match}}{\Longrightarrow} \begin{bmatrix} 6\text{ mo.} = 0 \\ 12\text{ mo.} = -1.11 \end{bmatrix} \end{bmatrix}$$

$$+ \begin{bmatrix} \text{Allograft} \overset{\text{Match}}{\Longrightarrow} \begin{bmatrix} 6\text{ mo.} = 0 \\ 12\text{ mo.} = 0.312 \end{bmatrix} \\ \text{Autograft} \overset{\text{Match}}{\Longrightarrow} \begin{bmatrix} 6\text{ mo.} = 0 \\ 12\text{ mo.} = -0.312 \end{bmatrix} \end{bmatrix}$$

Fig. 2.

Validation of the weighted least-squares regression model. A significant effect of graft type ($P = 0.001$) and a significant interaction between time point*graft type ($P = 0.016$) and time point*graft source ($P = 0.001$) were observed on the normalized MRI signal intensity. As such, the model is supported by the strong correlation between observed versus predicted values of normalized MRI signal intensity ($R^2 = 0.697$; $P < 0.001$). The coefficients for each level of the independent variables in the predicted normalized MRI signal intensity model are shown above

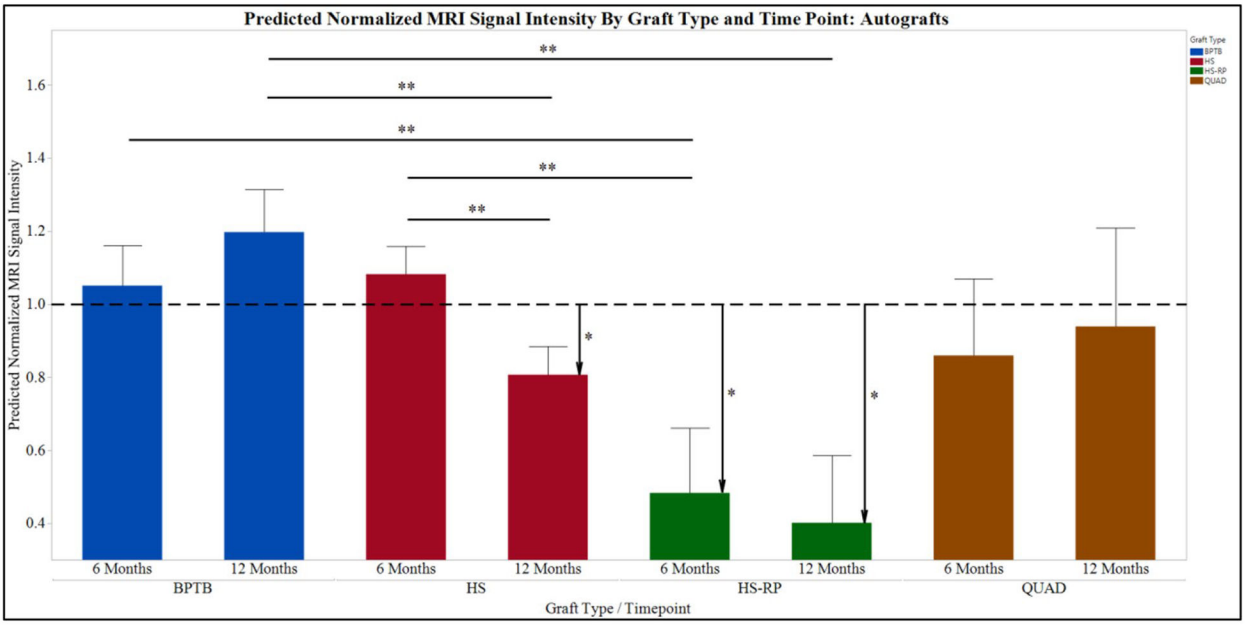

Fig. 3.

Predicted normalized MRI signal intensity by graft type and time point: autografts. HS-RP grafts were associated with decreased predicted normalized MRI signal intensity, an increased graft maturity, at all time points. Furthermore by 12 months postoperatively, predicted normalized MRI signal intensity was significantly greater in BPTB grafts compared to HS grafts without differences in HS versus HS-RP grafts (n.s.). These results suggest increasing graft maturation at 12 months in HS and HS-RP grafts compared to BPTB

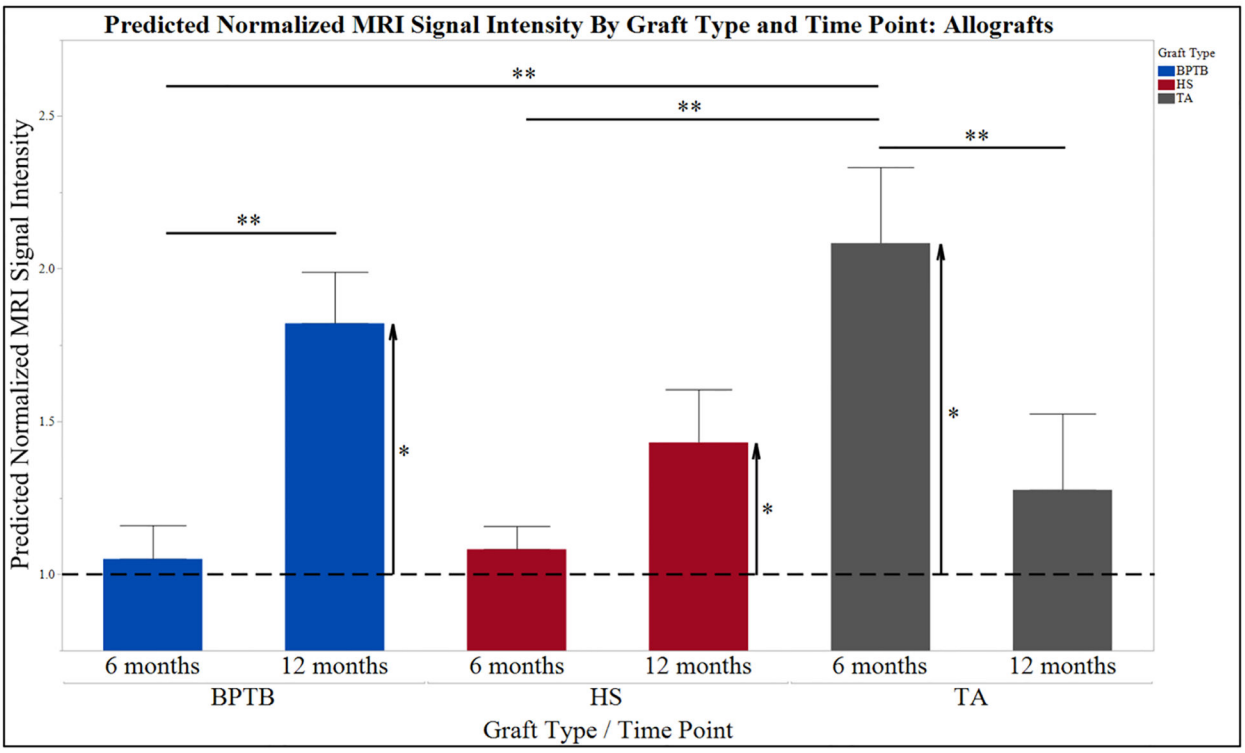

Fig. 4.

Predicted normalized MRI graft signal intensity by graft type and time point: allografts. Allograft source increased predicted normalized MRI signal intensity at 12 months postoperatively (Fig. 2). In contrast to HS and BPTB autografts, there was not a significant difference between HS and BPTB allografts at 12 months; both graft types at this time point were significantly increased above the normalized ratio of 1, indicating a decrease in maturity. Furthermore, between 6 and 12 months BPTB predicted normalized MRI signal intensity significantly increased, suggesting a decrease in graft maturation during this time

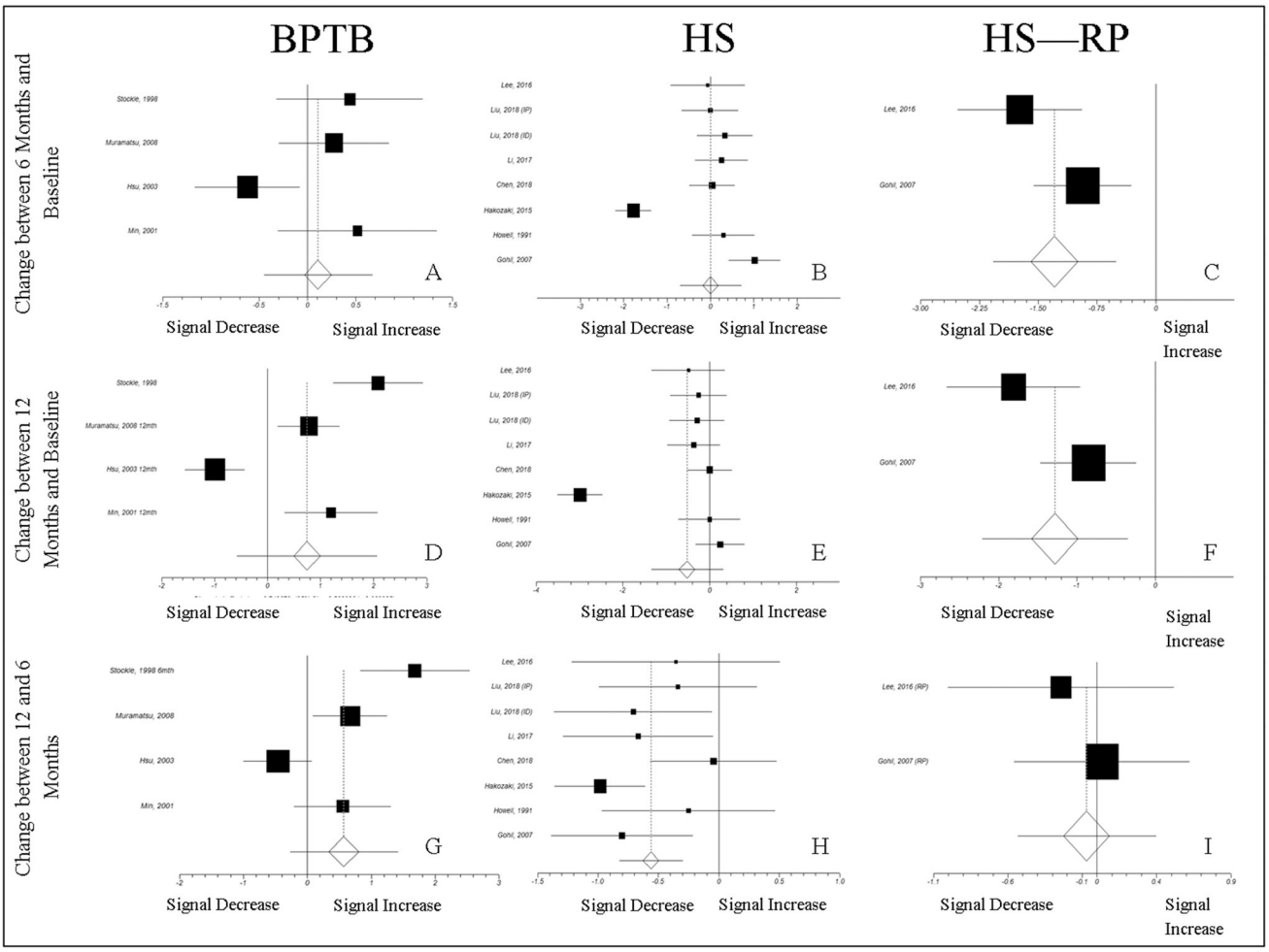

Fig. 5.

Normalized MRI Signal Intensity Effect Sizes: Changes from baseline 2 and between 6 and 12 Months. The trends in the effects of normalized MRI signal intensity parallel those predicted by the experimental model. In Panel E, the effect for the change between 12 months and baseline is not significant, while the model predicts a significant decrease in normalized MRI signal intensity for HS autografts from the ratio of 1 at 12 months (Fig. 3). The observed difference between the model and effect size calculation in this trend could be due to variability in the normalized MRI signal, accounted for in the effect size calculation, but not the 1-sample T-test used to assess predicted normalized MRI signal intensity change from baseline

Table 1

Literature search terms and study inclusion and exclusion criteria

Search terms					
Imaging	**“OR”**	**Graft**		**“OR”**	**Outcome**
Serial MRI		ACL	Hamstring	Quadriceps tendon	Healing
Magnetic resonance imaging		Anterior cruciate ligament	Hamstring graft	Quadriceps tendon graft	Outcomes
MRI		Patellar tendon	Hamstring tendon	Allograft	Reconstruction
MR		Patellar tendon graft	Hamstring tendon graft	Allograft tendon	Repair
Quantitative MRI		Bone–tendon–bone	Semitendinosus tendon	Autograft	
Signal/noise quotient		Bone–tendon–bone graft	Semitendinosus graft	Autograft tendon	
		Bone–patellar tendon–bone	Gracilis tendon		
		Bone–patellar tendon–bone graft	Gracilis tendon graft		

Inclusion criteria

1. Randomized controlled trials, case–control, cohort, or comparative studies
2. Reports of surgical outcomes following ACL reconstruction without complication
3. Use of MRI, focused on the intra-articular portion of the surgically implanted ACL graft
4. Multiple MRI imaging time points during the first postoperative year
5. English language

Exclusion criteria

1. Alternative organ system, disease process, or surgical procedure
2. Failure to quantify the intra-articular ACL signal on MRI following reconstructive surgery
3. Lack of ACL graft imaging using MRI at multiple postoperative time points
4. Lack of live human subjects
5. ACLR revision procedure to the affected knee
6. Use of functional imaging (dynamic/static contrast-enhanced MRI; magnetic resonance angiography) without reporting of pre-enhancement MRI signal intensities

Table 2

Characteristics of studies included in the least-squares regression model

Author	Intervention/ comparison; Level of Evidence	Study size	Graft (source)	Imaging parameters	SNQ calculation
Chen et al. [12]	Semitendinosus and gracilis (autograft) versus doublelooped fresh-frozen tendon (allograft) Level of Evidence: III	Autograft (N = 28: age: 29 ± 6 years); allograft (N = 20; age: 30±6 years)	(1) Semitendinosus and gracilis (autograft); (2) double-looped fresh-frozen tendon (allograft)	3.0T MRI: sagittal imaging with PD-Fs and 3D-DESS sequences	$\frac{\text{signal ACL graft} - \text{signal PCL}}{\text{background signal}}$ Evaluated at and femoral tunnel site and intra-articular tibial, mid-substance, and femoral graft sites
Gohil et al. [17]	Minimal debridement/ remnant preservation (RP) versus standard reconstruction Level of Evidence: I	RP (N = 22: age: 30.5 years, range: 15–59 years); standard (N = 24; age: 35.5 years, range: 21–50)	Double-looped semitendinosus and gracilis tendon (autograft)	1.5T MRI: TR/TE 3000/30 ms (PD-FSE); TR/TE 4000/85 ms (T2-FSE, fat suppressed); 3 mm slice thickness	$\frac{\text{signal ACL graft}}{\text{signal of background}}$ Evaluated near the femoral tunnel, graft mid-substance, near the tibial tunnel, and within tibial tunnel
Hakozaki et al. [18]	None (observational study) Level of Evidence: II	N = 61; age: 28.2 years, range: 13–48 years	Two double-looped semitendinosus tendons (autograft)	1.5T MRI: TR/TE 500/18 ms (T2*WI); TR/TE 2666/22 ms (PDWI); 15 cm field of view; 4 mm slice thickness	$\frac{\text{signal ACL graft(AMB or PLB)}}{\text{signal of PCL}}$ Evaluated at the entire intra-articular portion of the graft
Howell et al. [20]	Impinged versus unimpinged ACL grafts Level of Evidence: III	Impinged (N = 17; age: 23 years). Unimpinged (N = 15; age: 25 years)	Double-looped semitendinosus and gracilis tendon (autograft)	1.5T MRI: TR/TE: 1200/40 ms (standard spin-echo); 3 mm slice thickness	Raw ACL graft signal intensity. Evaluated at the proximal, middle, and distal portions of the intra-articular graft.
Hsu et al. [21]	None (observational study) Level of Evidence: IV	N = 27: age: 27.2 years, range: 18–45 years	Bone–patellar tendon-bone (autograft)	1.5T MRI	Raw ACL graft signal intensity. Evaluated in the middle of the graft.
Lee et al. [24]	Remnant preservation (RP) versus remnant sacrificing (RS) surgical techniques Level of Evidence: III	RP (N = 56; age: 30.1 years), RS (N = 42; age: 30.4 years)	Semitendinosus and gracilis tendon (autograft)	1.5T MRI: TR/TE 3000–4000/17–18 ms (PDWI)	$\frac{\text{signal ACL graft} - \text{signal of quadriceps tendon}}{\text{background signal}}$ Evaluated at proximal, middle, and distal portions of the anteromedial and posterolateral bundles of the ACL graft
Lee et al. [25]	None (observational study) Level of Evidence: IV	N = 247; age: 29 years, range: 18–58 years	Central quadriceps tendon–patellar bone graft (autograft)	1.0T MRI, 1.5TMRI: Tl, TW-SE, PD-FSE fat-saturated sequences	Intra-articular raw signal intensity evaluated at the proximal, middle, and distal portions of the graft *Note: data reported graphically as “signal intensity (ratio)”
Li et al. [26]	Double-looped semitendinosus and gracilis tendon (autograft) versus tibialis anterior (allograft) Level of Evidence: III	Autograft (N = 21; age: 29.5 ± 5.0 years), allograft (N = 17; age: 30.8 ± 5.9 years)	Double-looped semitendinosus and gracilis tendon (autograft); tibialis anterior (allograft)	3.0T MRI: TR/TE: 3000/28 ms (PD fat saturation); TR/TE: 5730/34 ms (STIR); TR/TE: 14.1/5 ms (3D-DESS); 15 cm field of view, slice thickness 3 mm (0.6 mm for 3D-DESS)	$\frac{\text{Signal ACL graft} - \text{signal of quadriceps tendon}}{\text{backgroud signal}}$ Evaluated as the average of the proximal, middle, and distal portions of the ACL graft
Liu et al. [30]	Semitendinosus and gracilis graft tibial insertion preservation	Insertion preservation (N = 18; age: 31.5 ± 6.6 years); insertion detachment (N = 19; age: 29.4±5.3 years)	Double-looped semitendinosus and gracilis tendon (autograft) with: tibial	3.0T MRI: TR/TE: 3000/28 ms (PD fat saturation); TR/TE: 5730/34 ms	$\frac{\text{Signal ACL graft} - \text{signal of quadriceps tendon}}{\text{backgroud signal}}$ Evaluated at the “graft site”

Author	Intervention/ comparison; Level of Evidence	Study size	Graft (source)	Imaging parameters	SNQ calculation
	versus tibial insertion detachment Level of Evidence: I		insertion preservation or tibial insertion detachment	(STIR); 15 cm field of view; 3 mm slice thickness	
Min et al. [32]	None (prospective observational cohort study) Level of Evidence: II	*N* = 23; age: 32 years, range: 16–54 years	Bone-patellar tendon-bone (autograft)	1.5T MRI: TR/TE: 20/70 (PDWI, T2WI); 14–18 cm field of view; 4 mm slice thickness	Raw signal intensity of the ACL graft
Muramatsu et al. [33]	Bone-patellar tendon-bone: allograft versus autograft Level of Evidence: III	Autograft (*N* = 20; age: 28.3 ± 6.3 years); allograft (*N* = 24; age: 26.1 ± 1.6 years)	Bone-patellar tendon-bone (autograft and allograft)	1.0T MRI: TR/TE: 500/17 ms (T1WI)	$\frac{\text{Signal ACL graft} - \text{signal of quadriceps tendon}}{\text{backgroud signal}}$ Evaluated at the center of the intra-articular region of the graft
Stockle et al. [38]	None (prospective observational study) Level of Evidence: II	*N* = 20; age 30 years, range: 17–59 years	Patellar tendon bone graft (autograft)	Native Tl/T2-weighted spin-echo (SE) sequences; contrast-enhanced (Gd-GTPA 0.1 mmol/kg body weight) dynamic gradient echo turbo flash sequences and Tl-SE and fat-saturation sequences	$\frac{\text{Signal ACL graft} - \text{signal of quadriceps tendon}}{\text{backgroud signal}}$ Evaluated at the proximal, middle, and distal thirds of the intra-articular graft in native T1 sequences and after Gd-GTPA contrast administration

Author	Imaging outcomes	Imaging follow-up	Imaging findings	Clinical outcomes/evaluations	Clinical follow-up	Quality score**
Chen et al. [12]	(1) SNQ; (2) Graft bending angle (angle between femoral bone tunnel and line connecting femoral and tibial tunnel openings)	Autograft and allograft groups: 3, 6, and 12 months	No significant differences were observed between HS allografts and autografts during the postoperative follow-up period	(1) IKDC; (2) Lysholm knee score; (3) Tegner knee score; (4) Anterior drawer test; (5) Lachman test	Uncertain	17 (8/1/6/1/1)
Gohil et al. [17]	(1) SNQ; (2) damage to PCL; (3) incidence of cyclops lesions; (4) assessment of impingement; (5) tibial tunnel placement; (6) femoral tunnel placement	2, 6, and 12 months	HS-RP autograft signal was significantly greater than HS autografts at 2 months and significantly less than HS autografts at 6 months postoperatively	(1) Knee swelling; (2) incidence of complications; (3) range of motion, measured with goniometer; (4) stability using KT-1000 arthrometer; (5) Lachman test; (6) IKDC score; (7) one-legged hop test	2 weeks, 2 months, 6 months, 12 months	21 (10/1/5/5/0)
Hakozaki et al. [18]	(1) SNQ	3, 6, and 12 months	MRI SNQ was significantly greater at 6 months compared to 3 and 12 months postoperative time points for HS autografts	(1) Lysholm score; (2) Tegner activity level; (3) IKDC score; (4) AP stability on KT-2000 arthrometer; (5) Pivot shift test	12 months	20 (10/2/5/3/0)
Howell et al. [20]	(1) ACL graft signal intensity; (2) tibial tunnel location	3, 6, and 12 months (impinged: 26.9 ± 8.9 months, unimpinged: 12.4± 1.7 months)	No significant differences in HS autograft MRI signal intensity was observed throughout the first postoperative year	(1) Knee extension; (2) pivot shift test; (3) knee laxity with KT-1000 arthrometer	12 months	15 (7/2/4/2/0)
Hsu et al. [21]	(1) ACL graft signal intensity; (2) tibial tunnel width at bone plug site and aperture; (3) tibial tunnel	3, 6, 12, and 18 months	A decreasing trend in MRI signal intensity throughout the first postoperative year was observed for BPTB autografts	None	N/A	14 (5/2/5/2/0)

Author	Imaging outcomes	Imaging follow-up	Imaging findings	Clinical outcomes/evaluations	Clinical follow-up	Quality score**
	length; (4) patellar tendon MRI signal; (5) patellar tendon thickness; (6) patellar tendon length					
Lee et al. [24]	(1) SNQ; (2) frequency of interbundle high signal intensity; (3) signal intensity of ACL remnant (evaluated in RP group)	< 1 month (RP: *N* = 10, RS: *N* = 10), 2–4 months (RP: *N* = 19, RS:N = 11), 6–9 months (RP: *N* = 15, RS: *N* = 10), 12–18 months (RP: *N* = 12, RS: *N* = 11)	HS-RP demonstrated increased MRI SNQ at 2–4 months compared to HS grafts. HS SNQ remained constant throughout the postoperative period while HS-RP SNQ decreased significantly from 2 to 4 months postoperatively	None	N/A	12 (5/1/4/2/0)
Lee et al. [25]	(1) ACL graft signal intensity ratio; (2) graft donor-site change; (3) merchant congruence angle; (4) Insall-Salvati ratio	3–6 months (*N* = 36), 7–12 months (*N* = 26), 13–18 months (*N* = 14), 19–24 months (*N* = 7), 25–30 months (*N* = 8),> 31 months (*N* = 7)	No significant differences in QUAD graft signal intensity ratio were observed between postoperative time points	(1) Second look arthroscopy, biopsy; (2) complications; (3) donor-site morbidity; (4) range of motion; (5) Lachman test; (6) anterior drawer test; (6) pivot shift test; (7) anterior laxity on KT-1000 arthrometer; (8) quadriceps muscle strength; (9) Lysholm knee score; (10) IKDC score; (11) Shelbourne and Trumper questionnaire	6 weeks, 3 months, 6 months, 9 months, 12 months, 18 months, 24 months, 30 months, and 36 months	18 (9/3/3/3/0)
Li et al. [26]	(1) SNQ; (2) presence of ligament tears and cartilage defects	3, 6, and 12 months	No significant differences in SNQ were observed between HS autografts and TA allografts during the postoperative period. Allograft SNQ was significantly increased at 6 months postoperatively	(1) IKDC score; (2) Lyshom Knee activity score; (3) Tegner activity score; (4) anterior drawer test; (4) Lachman test; (5) pivot shift test; (6) anterior tibial translation difference with KT-1000 knee arthrometer between healthy and reconstructed knees	3, 6, and 12 months	19 (9/1/5/3/1)
Liu et al. [30]	(1) SNQ	3, 6, 12, and 24 months	Preservation of the tibial bone insertion of HS grafts resulted in significantly decreased SNQ at 6 and 12 months postoperatively compared to standard HS graft ACLR	(1) Range of motion; (2) anterior drawer test; (3) Lachman test; (4) pivot shift test; 5	3, 6, 12, and 24 months	23 (10/1/7/5/0)
Min et al. [32]	(1) Signal intensity; (2) cross-sectional area of the graft	1, 2, 3, 6, and 12 months	Signal intensity at 12 months was significantly greater than 3 months postoperatively	None	N/A	12 (7/1/4/0/0)
Muramatsu et al. [33]	(1) SNQ (contrast-enhanced imaging was employed, raw values before and after enhancement were reported)	1, 4, 6, and 12 months	BPTB autograft SNQ was significantly greater than allograft SNQ at 4 and 6 months postoperatively. Allograft SNQ increased within the 4–12 months postoperative period while autograft signal remained relatively constant	None	N/A	17 (7/2/5/3/0)
Stockle et al. [38]	(1) Signal/noise ratio	2 weeks ± 3 days, 12 weeks ± 17 days, 24 weeks ± 42 days, year ± 49 days, 2 year ± 56 days	Sequential increase in graft signal/noise ratio throughout the first postoperative year was observed, decreasing by 2 years postoperatively	(1) Lysholm score; (2) OAK score; (3) IKDC score; (4) Lachman test; (5) pivot shift test; (6) KT-1000 laxity measurements; (7) range of motion (reported as flexion/ extension deficits)	6 months, 1 year, 2 years	14 (8/1/4/1/0)

** Subcomponent scores of reporting, external validity, internal validity—bias, internal validity—confounding, and power, respectively, are reported